



A Brief Overview of the Recent Bio-Medical Applications of Fiber Bragg Grating Sensors

Sharath Umesh^a and Sundarrajan Asokan^{a,b,*}

Abstract | Fiber Bragg Grating (FBG) sensors have become one of the most widely used sensors in the recent times for a variety of applications in the fields of aerospace, civil, automotive, etc. It has been recently realized that FBGs and etched FBGs can play an important role in biomedical applications. This article provides a brief overview of the recent advancements in the application of FBG sensors in bio-mechanical, bio-sensing and bio-medical fields.

1 Introduction

Fiber optic sensors have several advantages such as availability of large number of components from communication industry, small foot print, easy fabrication and immunity to Electromagnetic Interference (EMI).¹

In the category of fiber optic sensors, Fiber Bragg Gratings (FBGs) are desirable because of their high sensitivity, multi-modal sensing capability, large operational bandwidth and multiplexing capability.

A FBG is a periodic orthogonal perturbation of the refractive index along the longitudinal axis of the core of a single mode optical fiber. The periodic modulation of index of refraction is brought about by exploiting the photosensitivity of a germanium-doped silica fiber the optical fiber upon exposure to light.

The fabrication of FBGs has been first demonstrated by experiments conducted using visible Argon ion laser by Hill *et al.* and Kawasaki *et al.*^{2,3} However, the real breakthrough in the fabrication of FBGs has been achieved with the demonstration of the side writing technique by Meltz *et al.*⁴ Subsequently, various types of FBG inscription techniques, wherein higher refractive index changes brought about with ease and in shorter duration of time, have been reported.

FBGs, in the basic form, can sense strain and temperature.⁵ However, in recent years, several newer sensing applications of FBGs have been demonstrated. For example, in smart manufacturing, FBGs have been surface bonded or embedded in components during the manufacturing

process, and used to monitor parameters such as residual strain, pressure, viscosity, degree of cure, etc.⁶ FBGs have also been used in non-destructive evaluation to measure strain profiles and monitor delamination⁷. In civil engineering, FBG sensors have been used for mining, as well as structural health monitoring of tunnels, bridges and dams.⁸ In nuclear industry, they have been exploited for health monitoring of containment shells, cooling towers, steam pipes and storage sites. Further, FBGs have found applications in marine engineering particularly as underwater acoustic sensors.⁹ FBG sensors have also found application in aerospace engineering, in impact detection, cure processing, shape control and vibration damping.¹⁰

FBGs have shown a great potential for applications in the bio-medical field due to numerous advantages such as small size, non-toxicity, chemical inertness, etc.^{11,12} These features make FBG sensors apt for employment in both in vivo and in vitro measurements. Several books and review articles have been published, which discuss the utilization of FBG sensors in bio-medical applications.¹³⁻¹⁵ The current article is an attempt to provide a brief overview of the recent advancements in the bio-medical applications of FBG sensors, specifically in biomechanical, bio-sensing and bio-medical fields.

2 Fiber Bragg Grating Theory

As mentioned earlier, FBG is a periodic modulation of the refractive index of the core of a single-mode photosensitive optical fiber along its axis,¹⁶

^aDepartment of Instrumentation and Applied Physics, Indian Institute of Science, Bangalore, India.

^bApplied Photonics Initiative and Robert Bosch Center for Cyber Physical Systems, Indian Institute of Science, Bangalore, India.

*sasokan@iap.iisc.ernet.in
sundarrajan.asokan@gmail.com

established by exposing the core to an intensity-modulated UV light. When a broadband light is launched into a FBG, a single wavelength which satisfies the Bragg's condition is reflected back, and the remaining part of the spectrum is transmitted as shown in Figure 1.¹⁷ This reflected Bragg wavelength (λ_B) is given by

$$\lambda_B = 2 n_{eff} \Lambda \quad (1)$$

Here, Λ is the pitch of the grating and n_{eff} is the effective refractive index of the fiber core.

FBGs can be fabricated using a variety of ways. Some of the well known and widely used FBG fabrication methods include interferometric fabrication technique, point by point fabrication technique, phase mask fabrication technique and the mask image projection.⁵ The FBGs that are employed in all the applications described in the current review have been fabricated in photosensitive germania-doped silica fiber using the phase mask method.¹⁸

The sensing property of FBGs is based on the shift in resonance Bragg wavelength with a change in either the effective refractive index of the core or periodicity of the grating, effected by an external perturbation.

In general, the periodic spacing between the grating planes and the effective refractive index of the core are affected by ambient temperature and any axial strain on the fiber. By interrogating the shift in Bragg wavelength, the external perturbation at the grating site can be quantified.^{19,20} Using the Bragg condition (1), the shift in the Bragg wavelength due to strain and temperature is given by

$$\Delta\lambda_B = 2 \left[\Lambda \frac{\partial n_{eff}}{\partial l} + n_{eff} \frac{\partial \Lambda}{\partial l} \right] \Delta l + 2 \left[\Lambda \frac{\partial n_{eff}}{\partial T} + n_{eff} \frac{\partial \Lambda}{\partial T} \right] \Delta T \quad (2)$$

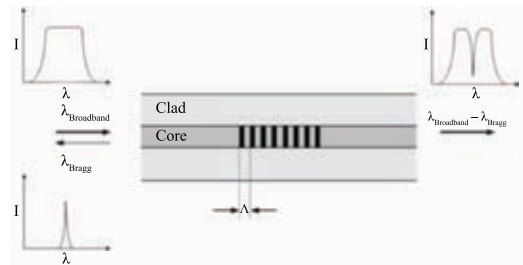


Figure 1: Working principle of fiber Bragg grating sensor.

The first term on the right side of (2) represents the strain effect on the change in the grating spacing and the strain-optic effect of the refractive index on the Bragg wavelength. The preceding strain effect term may be expressed as^{5,21}

$$\Delta\lambda_B = \lambda_B \left[1 - \frac{n_{eff}^2}{2} [p_{12} - \nu(p_{11} + p_{12})] \right] \epsilon_z \quad (3)$$

where p_{11} and p_{12} are components of the strain-optic tensor, ν is the Poisson ratio and ϵ_z is the strain. For a typical photosensitive fiber, 1.20 pm shift in the Bragg wavelength is observed upon applying 1 $\mu\epsilon$ over the FBG [5].

The second term on the right side of (2) represents the temperature effect on the change in the grating spacing and the temperature induced changes in the refractive index on the Bragg wavelength. This fractional wavelength shift for a temperature change ΔT can be expressed as^{5,21}

$$\Delta\lambda_B = \lambda_B (\alpha_\Lambda + \alpha_n) \Delta T \quad (4)$$

where α_Λ represents the thermal expansion coefficient and α_n represents the thermo-optic coefficient of the photosensitive fiber. In general, a shift in Bragg wavelength of 10pm is attained for a change in temperature of 1 K.⁵

3 Biomechanical Applications of FBG

3.1 Plantar strain measurement and postural stability analysis using FBG plantar strain sensing plate

A drastic increase in the occurrence of neuropathic or vascular ulceration in people has been noted in recent times. Peripheral neuropathy, together with vascular inefficiency, can lead the diabetic foot to physical ulceration that can further develop into gangrene resulting in the amputation of the

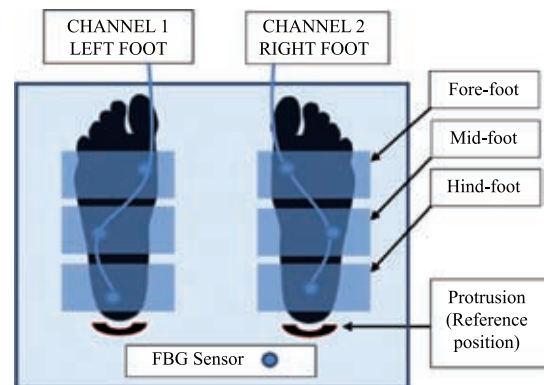


Figure 2: Schematic of the developed FBG plantar strain sensing plate.²⁶

leg.²²⁻²⁵ Damaged nerves in the foot of a person can cause balance impairment.^{26,27} Assessment of plantar strain distribution has gained importance in the identification of potential ulceration area in an individual.

Guru Prasad *et al.*²⁸ have recently demonstrated the deployment of FBG sensors for plantar strain measurements in the foot. This work focuses on the spatial resolution of the strain distribution in the foot at different regions such as fore-foot, mid-foot and hind-foot. It also quantifies with comparison, the postural stability of the subjects obtained from FBG sensors with centre of gravity movements obtained from tri-axial accelerometer.²⁹

The plantar strain sensing plate developed comprises of FBG sensors bonded between two perspex sheets as shown in Figure 2. Individual foot area is divided into three regions, namely fore-foot, mid-foot and hind-foot, and one FBG sensor is sandwiched between the Perspex sheets for each region. A single strand of fiber having three FBG sensors (of different Bragg wavelengths)

is deployed for each foot. The subjects are made to stand on the plantar strain sensing plate along with a tri-axial accelerometer attached at the second lumbar vertebra. The average strain obtained from the FBG sensors for the duration of the test is used for plantar strain distribution for individual subjects as shown in Figure 3; the variance of strain obtained is used for postural stability analysis for all the test subjects as shown in Figure 4.

An interesting outcome of the above study is the estimation of the maximum load application area of individual foot of 10 subjects, using the strain measurement from the plantar strain sensing plate. In addition, the postural stability of all the test subjects is compared with respect to both FBG plantar strain sensing plate and the accelerometer. The obtained results are found to be in good agreement, proving the efficient usage of FBG sensors for plantar strain measurement and postural stability analysis, which are important for designing specific shoe insoles for equal distribution of strain on the foot.

Foot pressure plates have been developed by various groups for dynamic strain sensing of foot using conventional sensors. Further, force plates have been developed to measure the three dimensional forces and the constituent moments using which the foot pressures can be extrapolated

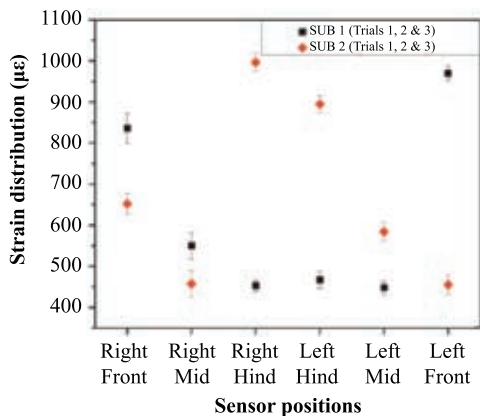


Figure 3: Plantar strain measured at different regions of foot for two individuals.²⁸

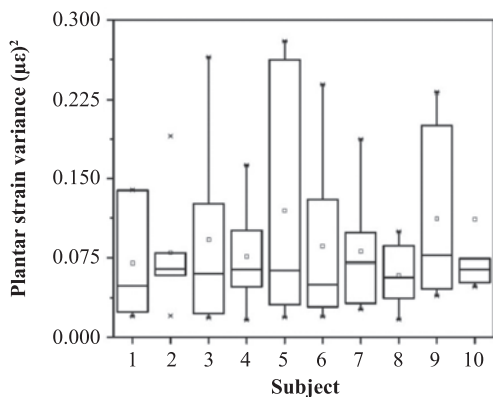


Figure 4: Strain variance computed for all subjects.²⁸

3.2 Airline exercise evaluation by FBG sensors, prescribed to avoid deep vein thrombosis

Immobility of body or body parts for long durations may subject one to the risk of Deep Vein Thrombosis (DVT), a situation where clots are formed in deep veins, obstructing the flow of blood in those parts.^{30,31} DVT in legs is a common situation encountered during long distance air travel.^{32,33} The anatomy of leg explains that the circulation of blood takes place with the arteries pumping blood from the heart and veins transporting blood to the heart (generally against gravity). The contraction and relaxation of the calf muscle provides the required force to pump the blood to the heart through the veins.³⁴ The assistance for blood circulation in lower limbs reduces the risk of DVT occurrence drastically. Hence, the leg exercises that induce the Calf Muscle Pump Activity (CMPA) and prevent the risk of DVT^{35,36} are generally prescribed. However, not all the exercises induce the required levels of CMPA, and hence may not be beneficial in prevention of DVT.^{37,38}

In this context, Guru Prasad *et al.*³⁹ have demonstrated a methodology of surface strain measurement on the skin of the calf muscle as an indicator of CMPA, to evaluate the usefulness of the prescribed exercises to avoid DVT. Ten exercises that are normally prescribed are shown in Figure 5. In addition, the authors have also suggested a new exercise and have carried out the same evaluation procedure as shown in Figure 6.

K. J. Donovan et al. evaluated the exercises suggested by recording the calf muscle pump activity with the aid of various sensing technologies such as surface electromyography, inertial sensors and magnetic sensors



Figure 5: Evaluated airline suggested exercises to avoid DVT.³⁹



Figure 6: New exercise suggested.³⁹

Three sensor methodologies have been used in the above experiments, with a repetition of each exercise 5 times for better accuracy. The FBG sensors are surface bonded on the medial belly of the right gastrocnemius for strain measurement. The strain recorded for one such exercise by an individual is shown in Figure 7. A Color Doppler Ultrasound (CDU) probe^{40,41} is positioned against the femoral vein of the thigh for blood velocity measurement. An Inertial Magnetic Unit (IMU) is employed to measure the acceleration and rotational attributes of the leg, which validates the repeatability of each exercise. The data from all the three sensor methodologies have been recorded simultaneously during the performance of each exercise by the subject for a sample size of 12.

It is inferred from the experiments performed that out of all the prescribed exercises, the exercise #1 and #6 are the most effective (Figure 8), based on the levels of strain obtained from FBG sensor as well as the blood velocity measured from the

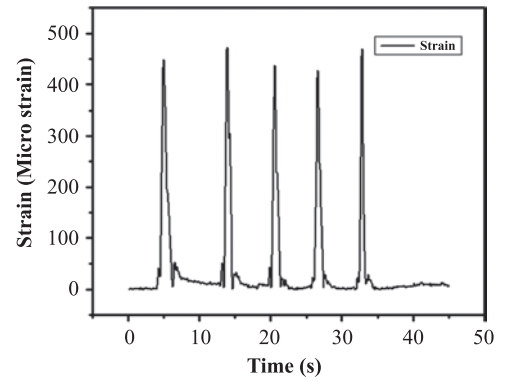


Figure 7: Strain recorded on the calf muscle by the FBG sensor during performance of exercise.³⁹

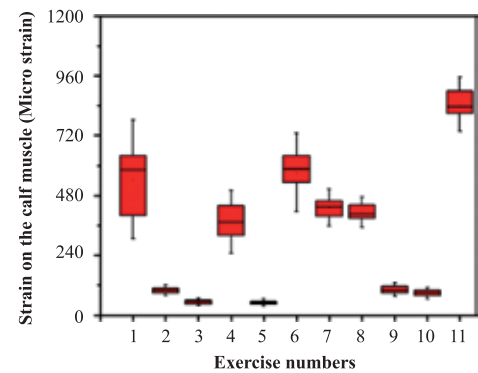


Figure 8: Compiled strain values measured for all subjects.³⁹

CDU probe. Using the data obtained from IMU, the repeatability of each exercise performed by individual subjects has been found to be good.

These studies also reveal that the suggested exercise #11 is better than the prescribed exercises, which is based on the highest strain measured by the FBG sensor and highest blood velocity measured from the CDU.

4 Bio-Sensing Applications of FBG

4.1 Etched fiber Bragg gratings coated with carbon nanotubes and graphene oxide along with a specific dendrimer

The use of Single walled carbon nanotubes (SWNTs) and graphene based Field Effect Transistors (FETs) for biological and chemical sensing applications are well known in literature.⁴²⁻⁴⁴ The detection of volatile organic compounds such as xylene and toluene by opto-chemical sensors (SWNT and its constituent nano composites deposited on optical fibers) by measuring the variation in reflectivity have also been established.⁴⁵

Further, mode-locking and bio-applications have been realized by selective area deposition of carbon nanotubes surrounding as well as at the tip end of the fibers using the reflectivity measurements.⁴⁶ In addition, assembly of polyelectrolyte molecules layer by layer on etched FBG (eFBG) by surface adsorption to estimate detection limit has been reported.⁴⁷

Recently, Sridevi S *et al.*⁴⁸ have demonstrated that etched Fiber Bragg Gratings (eFBGs) coated with Single Walled Carbon Nano-Tubes (SWNTs) and Graphene Oxide (GO) have high sensitivity, and can function as accurate biochemical sensors. The carbohydrate, mannose-functionalized poly(propyl-ether-imine) (PETIM) dendrimers (DMs) attached to the SWNT (or GO) coated eFBG have been used in the detection of specific and non-specific lectins, concanavalin A (Con A) and Peanut Agglutinin (PNA) respectively.

The ratio of shift in Bragg wavelength to Bragg wavelength has been reported to follow the Langmuir adsorption isotherm, with a high affinity constant of $4.2 \times 10^7 \text{ M}^{-1}$ for SWNT coated eFBG sensor and $3.4 \times 10^8 \text{ M}^{-1}$ for GO coated eFBG sensor.

The limit of detection for SWNT coated eFBG device obtained is 1 nM and the sensitivity for GO coated eFBG is 500 pM. eFBG coated with GO (functionalized with DM molecules) shows a higher specificity towards detection of Con A in the presence of excess amount of BSA protein.

The schematic of the coating procedure of SWNTs (or GO) is shown in Figure 9, and the Scanning Electron Microscopic image of GO coated eFBG in Figure 10.

Figure 11 shows the sensitivity response of different concentrations of only Con A, ConA mixed with 1.5 μM BSA, and only BSA to GO-DM complex coated eFBG.

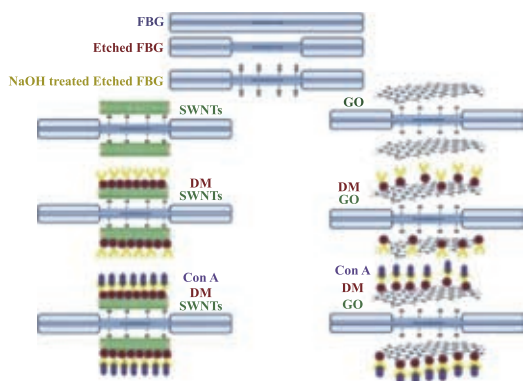


Figure 9: Schematic of coating of the GO, SWNTs on etched FBGs.⁴⁸

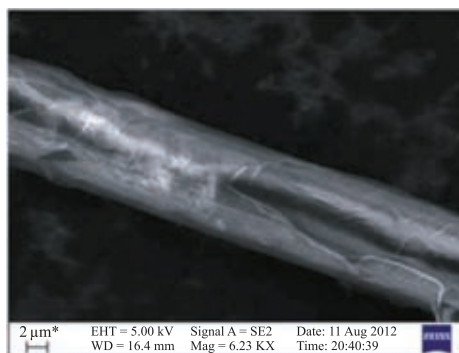


Figure 10: Scanning electron microscopic image of GO coated etched FBG.⁴⁸

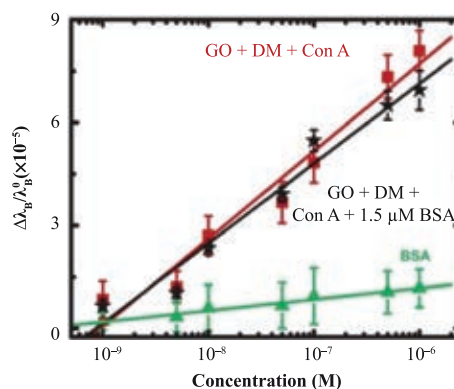


Figure 11: Response of the GO-DM coated eFBG dipped in different concentrations of only Con A, Con A mixed with 1.5 μM BSA and only BSA.⁴⁸

This study proves the efficacy of eFBG coated with SWNT or GO in the study of carbohydrate-protein interaction with multivalent specifically functionalized dendrimer acting as very sensitive biosensors. The methodology demonstrated is a platform technology that can be used for antibody-antigen interactions, bio- and chemical sensing applications.

5 Biomedical Applications

5.1 Blood pressure evaluation by arterial pulse waveform detection using fiber Bragg grating pulse device

It is an established fact that hypertension adversely affects the cardiovascular and renal systems.⁴⁹ Precise measurement of blood pressure is important as it can aid the diagnosis and management of hypertension. Due to its invasive nature, direct intra-arterial measurement of blood pressure, though being a gold standard method,⁵⁰ is not employed in clinical practice.^{51,52} Auscultatory method of obtaining the pressure from a

Dendrimers are macromolecules widely used to monitor many biologically relevant ligand-receptor interactions

Functionalized SWNT and GO coated on eFBG acts as a sensitive device for biological and chemical sensing due to the fact that the change in refractive index of the GO or SWNT coating is more than that of silica

The technique of blood pressure measurement using FBGPD can be made fully automated without any human intervention

sphygmomanometer, precisely at occurrence and disappearance of Korotkoff sounds during deflation of the Riva-Rocci cuff has been the mainstay for clinical measurement of blood pressure.⁵⁰ The occurrence and disappearance of Korotkoff sound is attributed to systolic blood pressure and diastolic blood pressure respectively.

Sharath *et al.*⁵³ have developed a Fiber Bragg Grating Pulse Device (FBGPD), which can record the Radial Arterial Pressure Pulse Waveform (RAPPW) comprising both beat-to-beat pulse waveform and arterial distension information together. The FBGPD developed has an FBG sensor bonded on the silicone diaphragm is in-turn, adhered to a hollow box and strap as shown in Figure 12.

The silicone facade of the FBGPD is wound to the wrist so that it positions the diaphragm bonded FBG sensor on the maximum impulse site of the pulsating radial artery. The radial artery striking the diaphragm causes strain variations,

which are sensed by the FBG sensor to provide the quantitative information of RAPPW of the subject as shown in Figure 13.

The sphygmomanometry test is carried out on a subject with the placement of FBGPD on the wrist together with an electronic stethoscope place on the ante-cubital fossa, as shown in the Figure 14. Data from both methodologies are simultaneously recorded throughout the test duration and compared with each other, and is shown in Figure 15.

The RAPPW recorded from FBGPD is divided into five distinct regions, namely normal pulsation, cuff inflation region, cuff deflation region, systolic to diastolic blood pressure region, and return to normalcy region accordingly. As the cuff deflates, the systolic blood pressure point is attributed to pulse detection in the radial artery, whereas the diastolic blood pressure point is attributed to maximal arterial distension in the RAPPW. A beat-to-beat coordination is established between the

Blood pressure measurement can be carried out by oscillometric devices, colin radial tonometer, vasotrac monitor and ultrasound techniques that are usually limited by accuracy of the algorithms employed



Figure 12: Photograph of FBGPD.⁵³



Figure 14: Simultaneous data acquisition from FBGPD and the electronic stethoscope during sphygmomanometry.⁵³

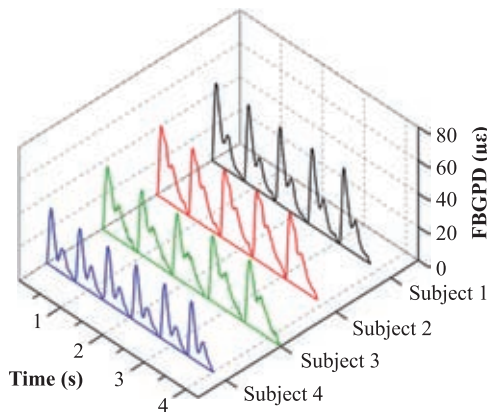


Figure 13: RAPPW response recorded using FBGPD.⁵³

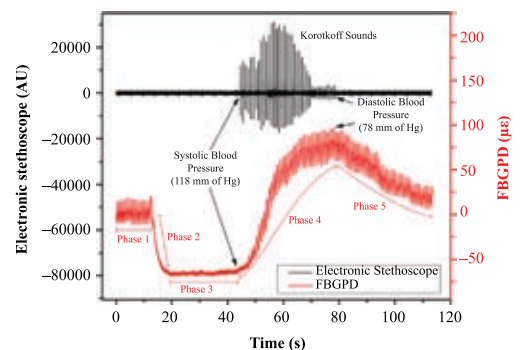


Figure 15: Comparison of response of FBGPD and electronic stethoscope signal during sphygmomanometry.⁵³

data obtained from FBGPD and electronic stethoscope in the systolic to diastolic blood pressure region (i.e. RAPPW and Korotkoff sounds). Both the systolic and diastolic blood pressure points obtained using the FBGPD and the electronic stethoscope are in good agreement within the acceptable accuracy percentages generated for a subject sample size of 60, which demonstrates the effective employment of FBG sensors for blood pressure evaluation.

5.2 In-vitro study for pulp chamber temperature variation using FBG thermal sensor

While cavity preparation and restorative procedures are carried out on a tooth, the dental pulp is found to be vulnerable due to the soft pulp tissue characteristics.⁵⁴ Polymerization of light-activated resin composites performed during restorative dental procedures causes an increase in the temperature of the pulp tissue.⁵⁵ The pulp vitality is reported to be compromised if the temperature of the pulp tissue is increased beyond 5–6 °C.^{55–57} An increase in temperature of pulp tissue occurs during polymerization of light composite resins owing to both the exothermic reaction process and the energy absorbed during irradiation.⁵⁸ Moreover,

during polymerization of composite resins, the extent of pulpal temperature rise is influenced by the intensity of the curing light used,⁵⁵ chemical composition of the restorative material,^{59,60} depth of the cavity or thickness of the restoration^{61,62} and irradiation duration.^{63,64}

The feasibility of using FBG sensors for pulp chamber temperature variation measurements has been shown by Sharath *et al.*,⁶⁵ in an in-vitro study during the polymerization of the composite resin induced by the light curing process for a Class I cavity. The FBG thermal sensor (FBGTS) has been designed for explicit temperature measurements, by sheathing the FBG sensor in a stainless steel tube (which transfers thermal variations onto the FBG sensor, and also protect it from other external perturbances) as shown in Figure 16. The FBG sensor element is positioned at the enclosed end of the FBGTS, while the other end is pigtailed to the connecting fiber.

A linear response for temperature increase has been observed between the FBGTS and the bare FBG sensor used for calibration. A Class I cavity of depth of 1.5 mm measured from the central groove is prepared on a tooth with the inverted cone diamond. 3M ESPE Z100 restorative composite (B2 shade) is used for packing of the prepared Class I cavity.

FBGTS has been introduced into the pulp chamber through the widened pulp canal, and the polymerization reaction is initiated by the external application light from a Woodpecker Blue Light Emitting Diode curing unit for a duration of 30 s as shown in Figure 17. This study reports an increase in temperature of 1.8 K during the light curing of the Class I filled composite resin as shown in Figure 18, which is within the acceptable range for the pulp tissue. The results obtained prove the effective usage of FBGTS for measurement of pulpal chamber temperature variations.

The diameter of the FBGTS has been reported as 150 μm which can enter into the pulp chamber via the pulp cavity (without much widening), helping to maintain the structural integrity of the tooth



Figure 16: Pictorial representation of FBGTS.⁶⁵

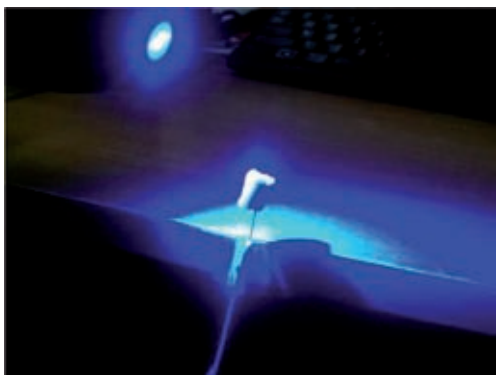


Figure 17: Light curing of Class I cavity.⁶⁵

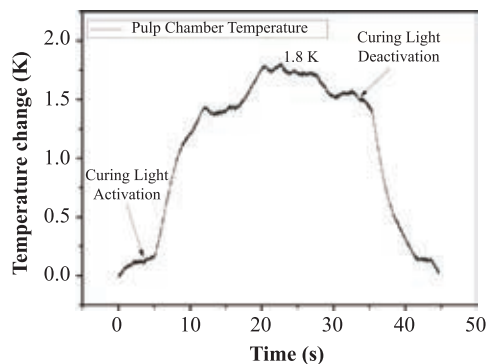


Figure 18: Temperature measured from FBGTS.⁶⁵

6 Summary

In this article, the recent developments in bio-medical applications of FBG sensors have been brought out. Some of the applications demonstrated are plantar strain measurement, exercise evaluation, bio-sensing by etched FBG with single walled carbon nanotube and graphene oxide coating, blood pressure estimation from arterial pulse pressure measurement and pulp chamber temperature variation measurement in a tooth. These examples clearly bring out the advantages of FBGs over the existing conventional technologies, in a wide range of bio-medical applications.

Acknowledgments

The authors would like to thank Prof AK Sood, Prof N Jayaraman, Dr SN Omkar, Dr GM Hegde, Dr AS Guruprasad, Dr KS Vasu, Mrs S Sridevi, Mrs K Chethana, Dr R Sukreet, Dr G Apoorva, Dr K Aadarsh, Dr B Adarsh, Dr NR Jayanth, Dr K Anand, Mr HN Vikranth and Mr V Anil, for their contribution in developing the individual applications which have been reviewed in the present article.

Received 13 August 2014.

References

1. B Lee, "Review of the present status of optical fiber sensors", *Opt. Fiber Technol.*, vol 9, pp 57–79, 2003.
2. K O Hill, Y Fujii, D C Johnson and B S Kawasaki, "Photosensitivity in optical fiber waveguides: Application to reflection filter fabrication", *Appl. Phys. Lett.*, vol 32, pp 647–649, 1978.
3. B S Kawasaki, K O Hill, D C Johnson and Y Fujii, "Narrow-band Bragg reflectors in optical fibers", *Opt. Lett.*, vol 3, pp 66–68, 1978.
4. G Meltz, W W Morey and W H Glenn, "Formation of Bragg gratings in optical fibers by a transverse holographic method", *Opt. Lett.*, vol 14, pp 823–825, 1989.
5. A Othonos and K Kalli, "Fiber Bragg Gratings: Fundamentals and Applications in Telecommunications and Sensing", Artech House, 1999.
6. C Caucheteur, F Lhommé, K Chah, M Blondel and P Mégret, "Simultaneous strain and temperature sensor based on the numerical reconstruction of polarization maintaining Fiber Bragg Gratings", *Opt. Las. Eng.*, vol 44, no 5, pp 411–422, 2006.
7. H Ling, K Lau, L Cheng and W Jin, "Viability of using an embedded FBG sensor in a composite structure for dynamic strain measurement", *Measurement*, vol 39, no 4, pp 328–334, 2006.
8. T H T Chan, L Yu, H Y Tam, Y Q Ni, S Y Liu, W H Chung and L K Cheng, "Fiber Bragg Grating sensors for structural health monitoring of Tsing Ma bridge: Background and experimental observation", *Eng. Struct.*, vol 28, no 5, pp 648–659, 2006.
9. F Xie, X Chen, L Zhang and M Song, "Realization of an effective dual-parameter sensor employing a single Fiber Bragg Grating structure", *Opt. Las. Eng.*, vol 44, issue 10, pp 1088–1095, 2006.
10. M Ussorio *et al.*, "Modifications to FBG sensor spectra due to matrix cracking in a GFRP composite, Construction and Building Materials", *Construction and Building Materials*, vol 20, no 1–2, pp 111–118, 2006.
11. C R Dennison, P M Wild, D R Wilson and P A Crompton, "A minimally invasive in-fiber Bragg grating sensor for intervertebral disc pressure measurements", *Meas. Sci. Technol.*, vol 19, pp 085201, 2008.
12. S J Mihailov, "Fiber Bragg grating sensors for harsh environments", *Sensors*, vol 12, pp 1898–1918, 2012.
13. V Mishra, N Singh, U Tiwari, P Kapur, "Fiber grating sensors in medicine: Current and emerging applications", *Sensor. Actuator. A Phys.*, vol 167, pp 279–290, 2011.
14. H J Kalinowski, "Fibre Bragg grating applications in Biomechanics", *Proc. SPIE*, vol 7004, pp 700430, 2008.
15. E Al-Fakih, N A A Osman and F R M Adikan, "The Use of Fiber Bragg Grating Sensors in Biomechanics and Rehabilitation Applications: The State-of-the-Art and Ongoing Research Topics", *Sensors*, vol 12, pp 12890–12926, 2012.
16. W W Morey, G Meltz and W H Glenn, "Fiber Bragg grating sensors", *Proc. SPIE*, vol 1169, pp 98–107, 1989.
17. A Othonos, "Fiber Bragg gratings", *Rev. Sci. Instrum.*, vol 68, no 12, pp 4309–4341, 1997.
18. K O Hill *et al.*, "Bragg gratings fabricated in monomode photosensitive optical fiber by UV exposure through a phase-mask", *Appl. Phys. Lett.*, vol 62, no 10, pp 1035–1037, 1993.
19. A D Kersey *et al.*, "Fiber grating sensors", *J. Lightwave Technol.*, vol 15, no 8, pp 1442–1462, 1997.
20. R Kashyap, "Fiber Bragg Gratings", Academic Press, San Diego, 1999.
21. G Meltz and WW Morey, "Bragg grating formation and germanosilicate fiber photosensitivity", *Proc. SPIE*, vol 1516, pp 185–199, 1991.
22. J Apelqvist and J Larsson, "What is the most effective way to reduce incidence of amputation in the diabetic foot?", *Diabetes Metab Res Rev.*, vol 16, pp 75–83, 2000.
23. P R Cavanagh, J S Ulbrecht and G M Caputo, "Biomechanical aspects of diabetic foot disease: Aetiology, treatment, and prevention", *Diabet. Med.*, vol 13, pp 17–22, 1996.
24. G E Reiber, "Who is at risk of limb loss and what to do about it?", *J Rehabil. Res. Dev.*, vol 31, pp 357–362, 1994.
25. A J Boulton *et al.*, "Dynamic foot pressure and other studies as diagnostic and management aids in diabetic neuropathy", *Diabetes Care*, vol 6, pp 26–33, 1983.
26. J Gareth, "The diabetic neuropathies: types, diagnosis and management", *J. Neurol. Neurosurg. Psychiatry*, vol 74, ii15, 2003.

27. E C Katoulis, ME Parry and S Hollis, "Postural instability in diabetic neuropathic patients at risk of foot ulceration", *Diabet. Med.*, vol 14, pp 296–300, 1997.
28. A S Guru Prasad, S N Omkar, H N Vikranth, V Anil, K Chethana and S Asokan, "Design and development of Fiber Bragg Grating sensing plate for plantar strain measurement and postural stability analysis", *Measurement*, vol 47, pp 789–793, 2014.
29. P Batista, P Oliveira and B Cardeira, "Accelerometer Calibration and Dynamic Bias and Gravity Estimation: Analysis, Design, and Experimental Evaluation", *IEEE Trans. Control Syst. Technol.*, vol 19, pp 1128–1137, 2011.
30. P Gispert *et al.*, "Economy-class syndrome or immobile Traveler's syndrome?", *Archivos De Bronconeumologia*, vol 42, no 7, pp 373–375, 2006.
31. Deep Vein Thrombosis Anatomical Chart, Anatomical Chart Company, Chicago, IL 2002.
32. K J Rothman, "Thrombosis after travel", *PLoS Med.*, vol 3, no 8, pp 1206–1207, 2006.
33. S C Cannegieter *et al.*, "Travel-related venous thrombosis: Results from a large population-based control study (MEGA study)", *PLoS Med.*, vol 3, no 8, pp 1258–1265, 2006.
34. K Hitos *et al.*, "Effect of leg exercises on popliteal venous blood flow during prolonged immobility of seated subjects: implications for prevention of travel-related deep vein thrombosis", *J. Thromb. Haemost.*, vol 5, no 9, pp 1890–1895, 2007.
35. British Airways, <http://www.britishairways.com/en-in/information/special-assistance/medical-conditions>
36. Continental Airways, <http://www.united.com/web/en-US/content/travel/inflight/health.aspx>
37. K J Donovan *et al.*, "Preliminary evaluation of recommended airline exercises for optimal calf muscle pump activity", *Eur. J. Vasc. Endovasc. Surg. Extra*, vol 12, no 1, pp 1–5, 2006.
38. K J Donovan *et al.*, "Accelerometer based calf muscle pump activity monitoring", *Med. Eng. Phys.*, vol 27, no 8, pp 717–722, 2005.
39. A S Guru Prasad, S J N Omkar, K Anand, GM Hegde and S Asokan, "Evaluation of airline exercises prescribed to avoid deep vein thrombosis using fiber Bragg grating sensors", *J. Biomed. Opt.*, vol 18, no 9, pp 097007, 2013.
40. W D Foley and S J Erickson, "Color Doppler flow imaging", *Am. J. Roentgenol.*, vol 156, no 1, pp 3–13, 1991.
41. R B Christopher and M D Merritt, "Doppler color flow imaging", *J. Clin. Ultrasound*, vol 15, no 9, pp 591–597, 1987.
42. H Vedalaet *et al.*, "Nanoelectronic detection of lectin-carbohydrate interactions using carbon nanotubes", *Nano Lett.*, vol 11, pp 170–175, 2011.
43. K S Vasu *et al.*, "Detection of sugar-lectin interactions by multivalent dendritic sugar functionalized single-walled carbon nanotubes", *Appl. Phys. Lett.*, vol 101, pp 053701, 2012.
44. Y Chen *et al.*, "Electronic detection of lectins using carbohydrate-functionalized nano-structures: graphene versus carbon nanotubes", *ACS Nano*, vol 6, pp 760–770, 2012.
45. C Andrea *et al.*, "Integrated development of chemoptical fiber nanosensors", *Curr. Anal. Chem.*, vol 4, pp 296–315, 2008.
46. K Kashiwagi and S Yamashita, "Deposition of carbon nanotubes around microfibervia evanescent light", *Opt. Express*, vol 17, pp 18364–18370, 2009.
47. B N Shivananju *et al.*, "Detection limit of etched fiber Bragg grating sensors", *J. Lightwave Technol.*, vol 31, pp 2441–2447, 2013.
48. S Sridevi, K S Vasu, N Jayaraman, S Asokan and A K Sood, "Optical bio-sensing devices based on etched fiber Bragg gratings coated with carbon nanotubes and graphene oxide along with a specific dendrimer", *Sensors and Actuators B*, vol 195, pp 150–155, 2014.
49. W C Cushman, "The burden of uncontrolled hypertension: morbidity and mortality associated with disease progression", *J. Clin. Hypertens.*, vol 5, no 3, pp 14–22, 2003.
50. M Ward and JA Langton, "Blood pressure measurement", *Contin. Educ. Anaesth. Crit. Care Pain.*, vol 7, no 4, pp 122–126, 2007.
51. D Perloff *et al.*, "Human blood pressure determination by sphygmomanometry", *Circulation*, vol 88 (5 Pt 1), pp 2460–2470, 1993.
52. D Sahu and M Bhaskaran, "Palpatory method of measuring diastolic blood pressure", *J. Anaesth. Clin. Pharmacol.*, vol 26, no 4, pp 528–530, 2010.
53. U Sharath, R Sukreet, G Apoorva, and S Asokan, "Blood pressure evaluation using sphygmomanometry assisted by arterial pulse waveform detection by fiber Bragg grating pulse device", *J. Biomed. Opt.*, vol 18, no 6, pp 067010, 2013.
54. S N Bhaskar and G E Lilly, "Intrapulpal temperature during cavity preparation", *J. Dent. Res.*, vol 44, pp 644–647, 1965.
55. M Hannig and B Bott, "In-vitro pulp temperature rise during composite resin polymerization with various light-curing sources", *Dent. Mater.*, vol 15, pp 275–281, 1999.
56. L Zach and G Cohen, "Pulp response to externally applied heat Oral Surg", *Med. Oral. Pathol.*, vol 19, pp 515–30, 1965.
57. K Langeland, "Effect of various procedures on the human dental pulp, Pulp reactions to cavity preparation and guttapurcha", *Oral Surg, Oral Med, and Oral Pathol*, vol 14, pp 210–33, 1961.
58. E K Hansen and E Asmussen, "Correlation between depth of cure and temperature rise of a light-activated resin", *Sc. and J. Dent. Res.*, vol 101, pp 176–179, 1993.
59. D S Cobb, D N Dederich, and T V Gardner, "In vitro temperature change at the dentin/pulpal interface by using conventional visible light versus argon laser", *Lasers in Sur. and Med.*, vol 26, no 4, pp 386–397, 2000.

60. A Knezevic *et al.*, "Degree of Conversion and temperature rise during polymerization of composite resin samples with blue diodes", *J. Oral Rehab.*, vol 28, pp 586–591, 2001.
61. L F Schneider *et al.*, "Halogen and LED light curing of composite: Temperature increase and Knoop hardness", *Clin. Oral Inv.*, vol 10, pp 66–71, 2006.
62. A R Yazici, A Muftu, G Kugel, and RD Perry, "Comparison of temperature changes in the pulp chamber induced by various light curing units, in vitro", *Oper. Dent.*, vol 31, pp 261–265, 2006.
63. H E Goodis, J M White, J Andrews, and L G Watanabe, "Measurement of temperature generated by visible-light-cure lamps in an in vitro model", *Dent. Mat.*, vol 5, pp 230–234, 1989.
64. D F Murchison and B K Moore, "Influence of curing time and distance on microhardness of eight light-cured liners", *Oper. Dent.*, vol 17, pp 135–141, 1992.
65. U Sharath, K Aadarsh, B Adarsh, NR Jayanth and S Asokan, "In-vitro measurement of temperature increase in pulp chamber with light cured composite resins using fiber Bragg grating thermal sensor", *Seventh International Conference on Sensing Technology (ICST)*, pp 235–237, 2013.



Mr. Sharath Umesh received his B.E. degree in Mechanical Engineering from Visvesvaraya Technological University, India in 2009. He is currently a Doctoral Student in the Department of Instrumentation and Applied Physics, Indian Institute of Science. His current research is based on packaging of FBG sensors for applications in various fields of engineering and medical sciences.



Prof. Sundarrajan Asokan received his M.Sc. degree in Materials Science from the College of Engineering, Anna University, Madras, India, and Ph.D. in Physics from the Indian Institute of Science, Bangalore, India. He is currently a Professor at the Department of Instrumentation and Applied Physics, Indian Institute of Science, and Chairman

of the Robert Bosch Centre for Cyber Physical Systems, Indian Institute of Science. He has published more than 180 papers in International Journals/Books. He is the recipient of The Martin J. Forster Gold Medal of the Indian Institute of Science for the best Ph.D. thesis in the division of Physical and Mathematical Sciences for the year 1986–1987, the Young Scientist Award of the Indian National Science Academy (1990), and the Young Scientist Research Award of the Department of Atomic Energy (1995), India. He was a JSPS Visiting Scientist at the Department of Electronics and Computer Engineering, Gifu University, Gifu, Japan, during 1991, INSA-Royal Society Visiting Scientist at the Imperial College of Science, Technology and Medicine, London, U.K., in 1998, and a Visiting Scholar at Lyman Laboratory, Harvard University, Cambridge, MA, in 1999. He is a Fellow of the National Academy of Sciences, India since 2008.